Journal of Anatomy

J. Anat. (2011) **219**, pp115–131 doi: 10.1111/j.1469-7580.2011.01388.x

Ontogeny of the cranial skeleton in a Darwin's finch (*Geospiza fortis*)

Annelies Genbrugge,[1,2] Anne-Sophie Heyde,[2] Dominique Adriaens,[2] Matthieu Boone,[3] Luc Van Hoorebeke,[3] Joris Dirckx,[1] Peter Aerts,[4,5] Jeffrey Podos[6] and Anthony Herrel[7]

[1]*Laboratory of Biomedical Physics, University of Antwerp, Groenenborgerlaan, Antwerpen, Belgium*
[2]*Evolutionary Morphology of Vertebrates, Ghent University, K.L. Ledeganckstraat, Gent, Belgium*
[3]*UGCT, Department of Physics and Astronomy, Ghent University, Institute for Nuclear Sciences (INW), Proeftuinstraat, Gent, Belgium*
[4]*Department of Biology, University of Antwerp, Universiteitsplein, Antwerpen, Belgium*
[5]*Department of Movement and Sports Sciences, Ghent University, Watersportlaan, Gent, Belgium*
[6]*Department of Biology and Graduate Program in Organismic and Evolutionary Biology, University of Massachusetts, Amherst, MA, USA*
[7]*Département d'Ecologie et de Gestion de la Biodiversité, Museum National d'Histoire Naturelle, 57 rue Cuvier, Case postale, Paris Cedex, France*

Abstract

Darwin's finches are a model system in ecological and evolutionary research, but surprisingly little is known about their skull morphology and development. Indeed, only the early beak development and external variation in adult beak shape has been studied. Understanding the development of the skull from embryo up to the adult is important to gain insights into how selection acts upon, and drives, variation in beak shape. Here, we provide a detailed description of the skeletal development of the skull in the medium ground finch (*Geospiza fortis*). Although the ossification sequence of the cranial elements is broadly similar to that observed for other birds, some differences can be observed. Unexpectedly, our data show that large changes in skull shape take place between the nestling and the juvenile phases. The reorientation of the beak, the orbit and the formation of well-developed processes and cristae suggest that these changes are likely related to the use of the beak after leaving the nest. This suggests that the active use of the jaw muscles during seed cracking plays an important role in shaping the adult skull morphology and may be driving some of the intra-specific variation observed in species such as *G. fortis*. Investigating the development of the jaw muscles and their interaction with the observed ossification and formation of the skull and lower jaw would allow further insights into the ecology and evolution of beak morphology in Darwin's finches.

Key words: cranial morphology; Darwin's finches; ontogeny.

Introduction

From a single common ancestor, 14 species of Darwin's finches have radiated throughout the Galapágos and Cocos Islands (Darwin, 1841; Grant, 1986). The near-perfect match between beak size and shape and diet in species specializing on different food resources has turned these finches into a classic textbook example of an adaptive radiation (Schluter & Grant, 1984). Three major groups of beak shapes with different functional specializations are typically distinguished: (i) deep and wide beaks of species that crush hard seeds; (ii) long and pointed beaks of species that probe flowers; and (iii) strongly curved upper and lower beaks of species that manipulate and bite food items at the tip of the beak (Bowman, 1961; Grant, 1986). More recently, Campàs et al. (2010) demonstrated that beak shape variation in Darwin's finches could be captured by three forms: (i) one for the ground finches; (ii) one for the tree finches; and (iii) one for the vegetarian finch. Within each class, beaks differ mainly through scaling and are thus highly similar in shape (see also Foster et al. 2008). Between shapes, shear transformations are, however, required to transform groups to a common shape (Campàs et al. 2010).

The adaptive nature of Darwin's finch beak shape is considered critically important to the survival of these animals, as during periods of food scarcity, animals with poorly suited beak shapes have lower survival (Boag & Grant, 1981). More-

Correspondence
Annelies Genbrugge, Evolutionary Morphology of Vertebrates, Ghent University, K.L. Ledeganckstraat 35, 9000 Gent, Belgium. T: ++32-9-264.52.20; F: ++32-9-264.53.44; E: annelies.genbrugge@ugent.be

Accepted for publication *8 April 2011*
Article published online *22 May 2011*

over, recent modeling efforts have demonstrated that beak shapes likely evolve in response to fracture avoidance (Soons et al. 2010). As such, beak size and shape can be considered adaptive. Moreover, beak shape is highly heritable (Schluter, 1984; Gibbs, 1988; Grant & Grant, 2006). Interestingly, recent developmental studies have demonstrated that most interspecific variation in beak size and shape in the ground finch clade can be explained by variation in gene expression associated with two distinct developmental pathways, with calmodulin expression driving variation in beak length and BMP4 expression regulating variation in beak width and depth (Abzhanov et al. 2004, 2006). Consistent with these observations, the shape of the beak in the ground finches, as defined by its scaling factor, appears to be correlated with expression levels of BMP4 (Campàs et al. 2010).

Whereas most of these previous studies on beak development focus explicitly on growth and ossification of the pre-nasal cartilage, an element crucial in the later development of the beak, surprisingly little is known about the development, ossification and growth of the rest of the cranial skeleton in these finches. Yet, to fully understand how selection acts upon, and drives, variation in beak shape, the growth and development of the cranial skeleton and its associated musculature must be understood in its entirety, as it is known that the interactions during development between muscles and bones are crucially important during development (Clabaut et al. 2009). Here we focus on the development of the cranial skeleton in the medium ground finch, *Geospiza fortis*, adding to the work of Grant (1981) and Abzhanov et al. (2004, 2006) on this species in providing a detailed description of development and ossification sequence of the cranium and hyobranchial apparatus from late embryo till adult. Considering that adults of this species are adapted for crushing hard seeds, structural modifications that arise during ontogeny reflecting the shift in diet hardness are also considered.

Materials and methods

Specimens

The analyzed material comprised 17 specimens of the medium ground finch (*Geospiza fortis*) of different size. These 17 specimens were grouped into four ontogenetic periods: (i) embryos (four specimens); (ii) nestlings (seven specimens); (iii) juveniles (two specimens); and (iv) adults (four specimens).

The embryos and nestlings were collected from abandoned nests on Santa Cruz Island in 2006. Nests were surveyed on a daily basis; eggs were collected from nests that were confirmed as abandoned, and nestlings were collected as soon as they were observed to be dead. Thus, all specimens were collected within maximally 18 h after death. The juvenile and adult specimens are road-killed specimens collected during February–March 2005 and 2006 on Santa Cruz Island. A stretch of road of approximately 5 km was walked continuously every day between sunrise and 13:00 hours, and all road-killed birds that showed no obvious external damage to the head were collected. Damage to specimens was verified afterwards using CT scans. Only intact specimens were used for our descriptions of cranial osteology. All embryos were collected at a single locality under a salvage permit from the Galápagos National Park Service. Embryos and nestlings were preserved overnight in a 5% aqueous formaldehyde solution, rinsed and transferred to a 70% aqueous ethanol solution. Juveniles and adults were preserved in a 10% aqueous formaldehyde solution for 24 h, rinsed and transferred to a 70% aqueous ethanol solution.

Of all specimens the head, beak, tarsus and wing dimensions were measured using digital calipers (Mauser digital, accuracy 0.01 mm) following Grant (1981) and Herrel et al. (2005a,b). Measurements included beak length, width and depth, head length, width and depth, tarsus length and wing chord. Of only three specimens the age is known, therefore, the specimens were ordered by their dimensions and ossification sequence (Tables 2 and 3).

CT scanning

The detailed descriptions of the osteology of the head and mandible are based on three-dimensional digital reconstructions. All specimens were scanned at the UGCT scanning facility at Ghent University (http://www.ugct.ugent.be). Reconstruction of the tomographic projection data was done using the in-house developed Octopus package (Vlassenbroeck et al. 2007). CT data were loaded into Amira 5.2.2 (64-bit version, Computer Systems Mercury) where the data were first reoriented along the *x*-, *y*- and *z*-axes so that all specimens are oriented along the same axes, which is necessary for constructing lateral images for morphometric analysis (see below). Bony structures were then identified semi-automatically based on gray-scale values of the voxels, with manual corrections to remove noise. To test whether CT scans give a correct indication of the ossification of the cranial skeleton, scans were compared with cleared-and-stained specimens of similar size. Volume and surface rendering were also performed in Amira 5.2.2. The anatomical nomenclature used in the descriptions is based on the Nomina Anatomica Avium (Baumel et al. 1979; Genbrugge et al. submitted).

Morphometrics

Five of the 17 specimens mentioned above were also used in a morphometric analysis. The three smallest specimens were not included in the analysis due to fractures or distortions of the skull. Two series of snapshots were taken in Amira 5.2.2. The first set comprises the left lateral view of the upper jaw and braincase (including the os pterygoideum and the os quadratum) of all five specimens (embryo 3, nestling 1 & 2, juvenile 1 and adult 1); a second set of images was taken of the left lateral view of the lower jaw. Using tpsDig2 2.16 (Rohlf, 2010b), we digitized two series of 18 homologous landmarks for the 'upper jaw + braincase' and seven homologous landmarks for the lower jaw (Table 1; Fig. 1). TpsSmall 1.2 (Rohlf, 2003) was used to perform a generalized least-squares Procrustes analysis where size, orientation and position are removed from the data set. TpsRelw 1.49 (Rohlf, 2010a) was then used to perform a PCA allowing us to explore the ontogenetic shape variation in *G. fortis*.

Shape changes of the lower jaw could not be fully captured using landmarks. Thus, we also performed an elliptical Fourier analysis on the outline of the lower jaws of the five specimens

Table 1 Description of the landmarks.

Number	Upper jaw + braincase: 18 landmarks
1	Distal tip of the os praemaxillare
2	Most rostral point of the nostril
3	Rostral point of fusion between the os nasale and the os praemaxillare
4	Most dorsal point of the nostril
5	Point of maximal curvature at frontonasal hinge
6	Point of fusion of the processus frontalis nasalis with the braincase
7	Point of maximum dorsal curvature of the orbit
8	Most dorsal point of the quadrato-squamosal articulation facet of the os squamosum
9	Most caudal point of the processus quadraticus of the os quadratojugale
10	Most ventral point of the processus quadraticus of the os quadratojugale
11	Most caudal point of the os palatinum
12	Most dorsal point of the pes pterygoidei of the os pterygoideum
13	Most rostral point of the os vomer
14	Caudal point of fusion between the os nasale and the os praemaxillare
15	Most caudal point of the processus maxillaris of the os praemaxillare
16	Most caudal point of the processus palatinus of the os praemaxillare
17	Point where the os maxillare enters the os praemaxillare
18	Point where the os palatinum enters the os praemaxillare
	Lower jaw: 7 landmarks
1	Rostral tip of the os dentale
2	Rostral point of maximal curvature of the foramen caudalis mandibulae
3	Caudal point of maximal curvature of the foramen caudalis mandibulae
4	Tip of condylus lateralis of the processus lateralis mandibulae
5	Tip of condylus caudalis of the processus lateralis mandibulae
6	Tip of processus retroarticularis
7	Most caudal point of the symphysis mandibulae

using the program 'Shape' (ChainCoder, CHC2NEF and PrinComp; Iwata & Ukai, 2002).

Results

Osteology

The detailed cranial osteology and ossification sequence is described below and summarized in Table 2. Scans of specimens of similar size were examined and deviations from the patterns described below are noted. A summary of all measurements (head length, head width, head depth, beak length, beak width, beak depth, tarsus length and wing chord) is provided in Table 3. Note that even though specimens are described and ordered based on their cranial size, variation in size may not correlate fully to variation in age (especially in the highly variable species *G. fortis*), and thus care should be taken in the interpretation of the ossification sequence, especially for the smallest two embryos.

Group 1: embryos

Embryo size 1 – HL 8.9 mm

The first embryo is similar to the oldest embryo used by Abzhanov (Abzhanov et al. 2004, 2006), but unfortunately this specimen is damaged. However, even though the beak is broken and bent ventrolaterally, it allows us to distinguish the bony elements present and thus provides a reference for our study of the ossification sequence (Figs 2 and 9; Tables 2 and 3).

Two bones of the braincase are already present: the os squamosum and the os parasphenoidale. The os squamosum has a triangular shape with one corner oriented rostrodorsally, one rostroventrally and one dorsocaudally. Its ventral side shows a concavity that will later be involved in the articulation of the squamosum with the upper head of the os quadratum. From the os parasphenoidale, only the rostrum parasphenoidale is visible as a small splint of bone, of which the caudal base is broader than the distal tip. It lies at the midline of the skull, dorsal to the os palatinum and the os pterygoideum.

The upper beak comprises three bones: the os praemaxillare, the os nasale and the os maxillare. The left and right ossa praemaxillaria are fused along the midline. The dorsal processus frontalis is formed by the fusion of both praemaxillary bones, which remain separated only at their proximal tip. The formation of the processus palatinus has started together with the ossification of the processus maxillaris, which extends somewhat more caudally than the former. Lateral to the processus frontalis praemaxillae, the os nasalis has started to ossify. It is a small sheet of bone running lateroventrally. The long os maxillare lies between the processus maxillaris praemaxillae and the processus palatinus praemaxillae, running further caudally. Its distal and proximal third are narrow and round in cross-section, and form the processus praemaxillaris and processus jugalis, respectively. The broader medial part consists of the dorsoventrally flattened and slender processus maxillopalatinus, which runs mediocaudally. The proximal third forms the jugal arch, together with the more caudally situated os quadratojugale. The latter is a long and slender bone that at its proximal end already has a visible condylus quadraticus, which is turned slightly medially.

The os palatinum is a wing-like structure, situated lateral, mediolateral and rostral to the slender rostrum parasphe-

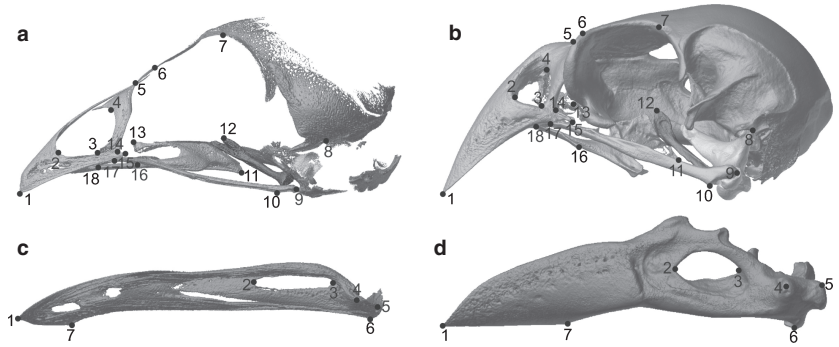

Fig. 1 Position of the landmarks in the embryo 3 (a,c) and the adult (b,d). An explanation of the landmarks is provided in Table 1.

noidale. A very well-developed processus praemaxillaris runs rostrally towards the ventromedial side of the os praemaxillaris, medial to the processus palatinus praemaxillae and ventral to the processus maxillopalatinus.

The os pterygoideum is a long slender bone that is round in cross-section. Its distal end is situated lateral to the rostrum parasphenoidale and consists of two rostrodorsally pointing spines. The lateral and longest spine runs

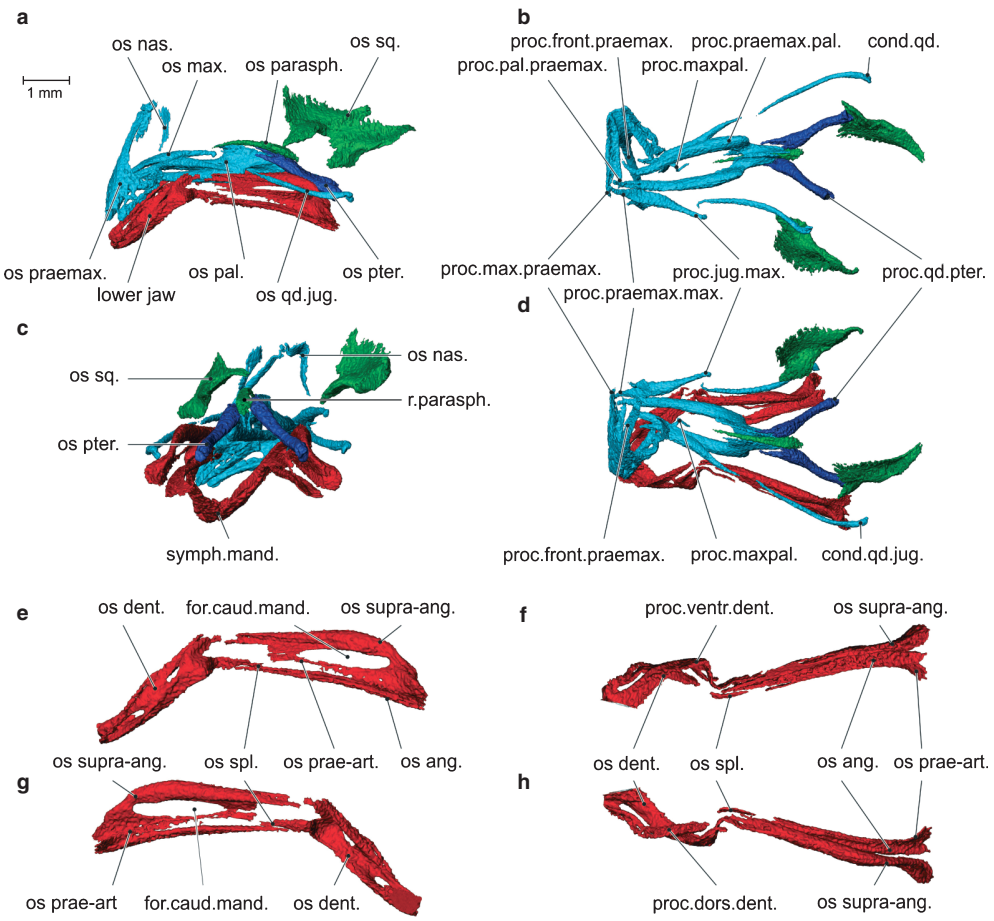

Fig. 2 Lateral view (a), ventral view (without lower jaw) (b), caudal view (c) and dorsal view (d) of the skull of embryo 1, and lateral view (e), ventral view (f), medial view (g) and dorsal view (h) of the left ramus of the lower jaw of embryo 1. Note that all the bones of the lower and upper jaw are present, but only two bones of the braincase have started to ossify. The beak of this specimen is broken and bent ventrolaterally. cond.qd.jug., condylus quadrati jugalis; for.caud.mand., foramen caudalis mandibulae; os ang., os angulare; os dent., os dentale; os max., os maxillare; os nas., os nasale; os pal., os palatinum; os qd.jug., os quadratojugalis; os parasphen., os parasphenoideum; os prae-art., os praearticulare; os praemax., os praemaxillare; os pter., os pterygoideum; os spl., os spleniale; os sq., os squamosum; os supra-ang., os supra-angulare; proc.dors.dent., processus dorsalis dentalis; proc.front.praemax., processus frontalis praemaxillae; proc.jug.max., processus jugalis maxillae; proc.max.praemax., processus maxillaris praemaxillae; proc.maxpal., processus maxillopalatinus; proc.pal.praemax., processus palatinus praemaxillae; proc.praemax.max., processus praemaxillaris maxillae; proc.praemax.pal., processus praemaxillaris palatini; proc.qd.pter., processus quadraticus pterigoidei; proc.ventr.dent., processus ventralis dentalis; r.parasph., rostrum parasphenoideum; symph.mand., symphysis mandibulae.

Table 2 Overview of the development of the different parts of the skull of the seven specimens.

	embr 1 DV09E03	embr 2 DV09E07	DV09E11	embr 3 DV09E06	DV09E10 4–5 days	DV09E08 5 days	DV09E09 7 days	DV09E02	DV09E05	nestl 1 DV09E04	nestl 2 DV09E01	juvenile DV09J02	DV09J01	adult DV09A01
os squamosum	x	x	x	x	x	x	x	x	x	x	x	x	x	x
os parasphen.	x	x	x	x	x	x	x	x	x	x	x	x	x	x
os basisphen.		x	x	x	x	x	x	x	x	x	x	x	x	x
os orbitosphen.					x	x	x	x	x	x	x	x	x	x
os pro-oticum				x	x	x	x	x	x	x	x	x	x	x
os opistoticum				x	x	x	x	x	x	x	x	x	x	x
os epioticum											x	x	x	x
os basioccipitale				x	x	x	x	x	x	x	x	x	x	x
os exoccipitale				x	x	x	x	x	x	x	x	x	x	x
os supraoccip.					x	x	x	x	x	x	x	x	x	x
os parietale				x	x	x	x	x	x	x	x	x	x	x
os frontale			x	x	x	x	x	x	x	x	x	x	x	x
os mesethmoid						x	x	x	x	x	x	x	x	x
os nasale	x	x	x	x	x	x	x	x	x	x	x	x	x	x
os praemaxillare	x	x	x	x	x	x	x	x	x	x	x	x	x	x
os maxillare	x	x	x	x	x	x	x	x	x	x	x	x	x	x
os palatinum	x	x	x	x	x	x	x	x	x	x	x	x	x	x
os vomer		x	x	x	x	x	x	x	x	x	x	x	x	x
os pterygoideum	x	x	x	x	x	x	x	x	x	x	x	x	x	x
os quadratojug.	x	x	x	x	x	x	x	x	x	x	x	x	x	x
os quadratum				x	x	x	x	x	x	x	x	x	x	x
os dentale	x	x	x	x	x	x	x	x	x	x	x	x	x	x
os supra-ang.	x	x	x	x	x	x	x	x	x	x	x	x	x	x
os angulare	x	x	x	x	x	x	x	x	x	x	x	x	x	x
os prae-art.	x	x	x	x	x	x	x	x	x	x	x	x	x	x
os articulare						x	x	x	x	x	x	x	x	x
os spleniale	x	x	x	x	x	x	x	x	x	x	x	x	x	x
os entoglossum				x	x	x	x	x	x	x	x	x	x	x
os basihyale									x		x	x	x	x
os urohyale								x			x	x	x	x
os ceratobranch.		x	x	x	x	x	x	x	x	x	x	x	x	x
os epibranchiale												x	x	x

'x' indicates the presence of a bone.

Table 3 Head and beak dimensions, tarsus length and wing chord of the specimens studied here. Specimens are ordered in accordance to their ossification sequence (see Table 2).

	embr 1	embr 2		embr 3						nestl 1	nestl 2	juvenile	
	DV09E03	DV09E07	DV09E11	DV09E06	DV09E10	DV09E08	DV09E09	DV09E02	DV09E05	DV09E04	DV09E01	DV09J02	DV09J01
Tarsus length	NA	4.37	3.74	6.12	9.39	11.70	NA	15.56	15.48	14.63	19.34	23.74	20.42
Wing chord	4.06	4.64	NA	5.79	6.47	11.62	NA	18.72	19.72	19.27	28.77	64.73	64.34
Head length	8.89	11.14	9.76	13.64	14.85	17.06	18.04	20.07	20.15	20.56	22.84	31.96	31.70
Head width	4.08*	4.98*	4.39	7.85	8.45	9.53	10.19	11.12	10.25	11.12	13.03	15.60	14.68
Head depth	5.27*	5.56*	4.22	6.94	8.95	9.65	10.78	10.63*	10.11	11.50	13.33	15.84	16.64
Beak length	3.61*	3.85	3.51	5.97	6.29	6.67	6.49	8.34	8.11	8.52	9.52	16.39	16.12
Beak width	2.06*	2.00	1.90	3.35	3.81	4.15	4.06	5.33	4.58	4.54	4.61	9.21	7.63
Beak depth	2.32*	3.19	2.57	3.74	3.71	3.78	3.86	5.01	4.24	4.70	5.59	11.06	11.39

Table entries are dimensions in mm.
*Due to fractures and distortions of the beak and/or head, these measurements should be treated with caution; NA, not available or not measureable.
For dimensions of adult specimens see Herrel et al. (2005a).

laterodorsally to the dorsocaudal edge of the os palatinum. The dorsal and smaller spine lies medial to the first one and runs dorsally to the caudal edges of the os palatinum. At the proximal end of the os pterygoideum the processus quadraticus is already distinguishable, and will form the articulation with the os quadratum.

The lower jaw comprises five bones, i.e. the os dentale, os angulare, os supra-angulare, os spleniale and os prae-articulare. Only the os articulare has not developed yet in this specimen. The rostral half of the lower jaw is formed by the os dentale. Left and right dental bones are partly fused at the midline to form the symphysis mandibulae. The processus dorsalis dentalis runs caudally towards the os supra-angulare, while the processus ventralis dentalis runs even more caudally towards the os angulare. The os supra-angulare is the largest bone of the caudal half of the lower jaw (pars caudalis). Its dorsal part is thick and forms the dorsal and dorsolateral part of the pars caudalis. The lateroventral part of this bone is slender and does not extend far rostrally. Both parts enclose the foramen caudalis mandibulae. At the caudal end of the os supra-angulare the formation of the quadrate-mandibular joint becomes apparent. Ventromedial to the os supra-angulare lies the os angulare. It is a long bone that makes up the whole ventral side of the pars caudalis. Its distal tip lies medial to the processus ventralis dentalis. Dorsomedial to this distal tip and medial to the processus ventralis dentalis a very thin and small os spleniale is situated. At its caudal end, the os angulare is slightly fused with the dorsomedially situated and thin os prae-articulare. Rostral to this fusion the os prae-articulare extends forward as a thin, long splint of bone that runs parallel to the os angulare positioned ventral to it.

Embryo size class 2 – HL 9.8 & 11.1 mm

The skull of these specimens (Figs 3 and 9; Tables 2 and 3) is slightly distorted, causing the ossa nasalis, os praemaxillare and ossa squamosa to be twisted relative to the other bony elements of the skull.

Apart from a continued uniform growth, the os squamosum has not changed qualitatively from the prior size class. The os parasphenoideale now has two additional centers of ossification, which form the left and right lamina basiparashenoidalis as two long plates oriented mediolaterally. The rostrum parasphenoidale has extended caudally but has not qualitatively changed in shape. In between the rostrum parasphenoidale and the laminae basiparasphenoidalis, the ossification of the os basisphenoidale has started. Dorsocaudal to each lamina basiparasphenoidalis lies the horseshoe-like macula lagenae. Caudomedial to the caudal tip of the os squamosum a small and round macula utriculi can be observed, with ventral to it a smaller, shell-like macula sacculi. The onset of ossification of the os frontale was visible in one specimen (DV09E11; Table 2).

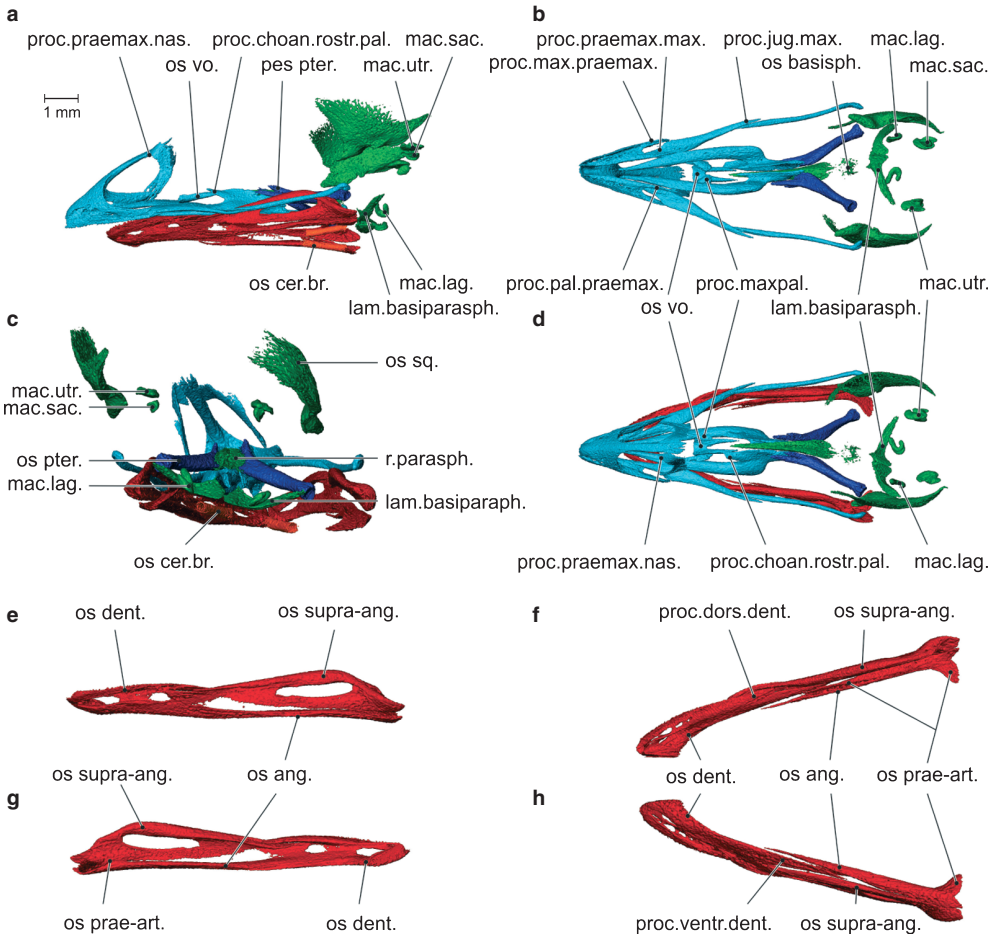

Fig. 3 Lateral view (a), ventral view (without lower jaw) (b), caudal view (c) and dorsal view (d) of the skull of embryo 2, and lateral view (e) and medial view (g) of the left ramus of the lower jaw and dorsal view (f), and ventral view (h) of the right ramus of the lower jaw of embryo 2. Note the start of the ossification of the hyoid apparatus. Dorsal and ventral views of the lower jaw were taken from the right ramus due to the small distortion of the left ramus. The os spleniale is not visible in this figure. It was observed on the CT data, but was so thin that smoothing during the reconstruction made it disappear. lam.basiparasph., lamina basiparasphenoidalis; mac.lag., macula lagenae; mac.sac., macula sacculi; mac.utr., macula utriculi; os ang., os angulare; os basisphen., os basisphenoideum; os cer.br., os ceratobranchiale; os dent., os dentale; os prae-art., os prae-articulare; os pter., os pterygoideum; os sq., os squamosum; os supra-ang., os supra-angulare; os vo., os vomer; pes pter., pes pterygoidei; proc.choan.rostr.pal., processus choanalis rostralis palatini; proc.dors.dent., processus dorsalis dentalis; proc.jug.max., processus jugalis maxillae; proc.max.praemax., processus maxillaris praemaxillae; proc.maxpal., processus maxillopalatini; proc.pal.praemax., processus palatinus praemaxillae; proc.praemax.max., processus praemaxillaris palatini; proc.praemax.nas., processus praemaxillaris nasalis; proc.ventr.dent., processus ventralis dorsalis.

The processus maxillaris and palatinus of the os praemaxillare now extend more caudally, with the former extending somewhat further caudad than the latter. The os nasalis has grown in a rostrolateral direction and its processus praemaxillaris nasalis can now be distinguished. This process runs rostrally, lateral to the processus frontalis praemaxillaris. The processus praemaxillaris maxillae has grown more rostrally and runs dorsal to the ventral side of the os praemaxillare, dorsorostral to the processus palatinus praemaxillae. The processus maxillopalatinus has extended caudally and has developed a flag-shaped caudal sheet. The processus jugalis maxillae and the os quadratojugale have grown towards each other such that the caudal tip of the os maxillare runs lateroventral to the distal tip of the os quadratojugale.

The os palatinum has developed a processus choanalis rostralis, running rostrolateral to the rostrum parasphenoidale and laterodorsal to the newly formed os vomer. On its ventral side, the os palatinum has developed a rostral spine. The processus praemaxillaris palatini has grown rostrally in between the two ventral halves of the os praemaxillare. The os vomer consists of two small, bilateral splints, of which the rostral halves have fused at the midline. The gutter-shaped os vomer lies rostroventral to the processus choanalis rostralis palatini and dorsomedial to the processus maxillopalatinus.

The medial rostrodorsal spine of the os pterygoideum has grown more rostrally and ventrally, giving it a more plate-like shape. This is the start of the formation of the pes pterygoidei.

The processus ventralis of the os dentalis now extends more caudally and lies between the os angulare and the os supra-angulare. The os supra-angulare has grown rostrally, with its distal tip enclosed by the processus dorsalis and the lateral surface of the os dentalis. The lateroventral part of the os supra-angulare has grown more rostrally and ventrally towards the os angulare. The caudal tips of the os supra-angulare, os angulare and os prae-articulare now extend more caudally to form the processus retroarticularis. The rostral part of the os prae-articulare is more ossified.

The ossi ceratobranchiale have started to ossify as two ossifying bars of perichondral origin.

Embryo size 3 – HL 13.6 mm

By this size class, the os squamosum has grown and makes contact rostrodorsally with the newly formed os frontale and caudally with the newly formed os parietale. The os frontale forms the dorsal roof of the orbit. Its rostral tip lies caudal to the newly formed processus frontalis nasalis; its ventrocaudal edge runs medial to the rostrodorsal tip of the os squamosum. At the base of the skull four new bones have started to form: the os basioccipitale, the os exoccipitale, the os opisthoticum and the os prooticum. The dorsal and ventral sides of the perichondral os basioccipitale have started to form and lie as two oblong plates along the midline on the ventral side of the skull. Laterocaudal to the os basioccipitale lies the perichondral os exoccipitale, which has an irregular shape. On its rostrodorsal side an only very slightly ossified os opisthoticum is visible. Ventromedial to the os squamosum and rostrodorsal to the maculae utriculi

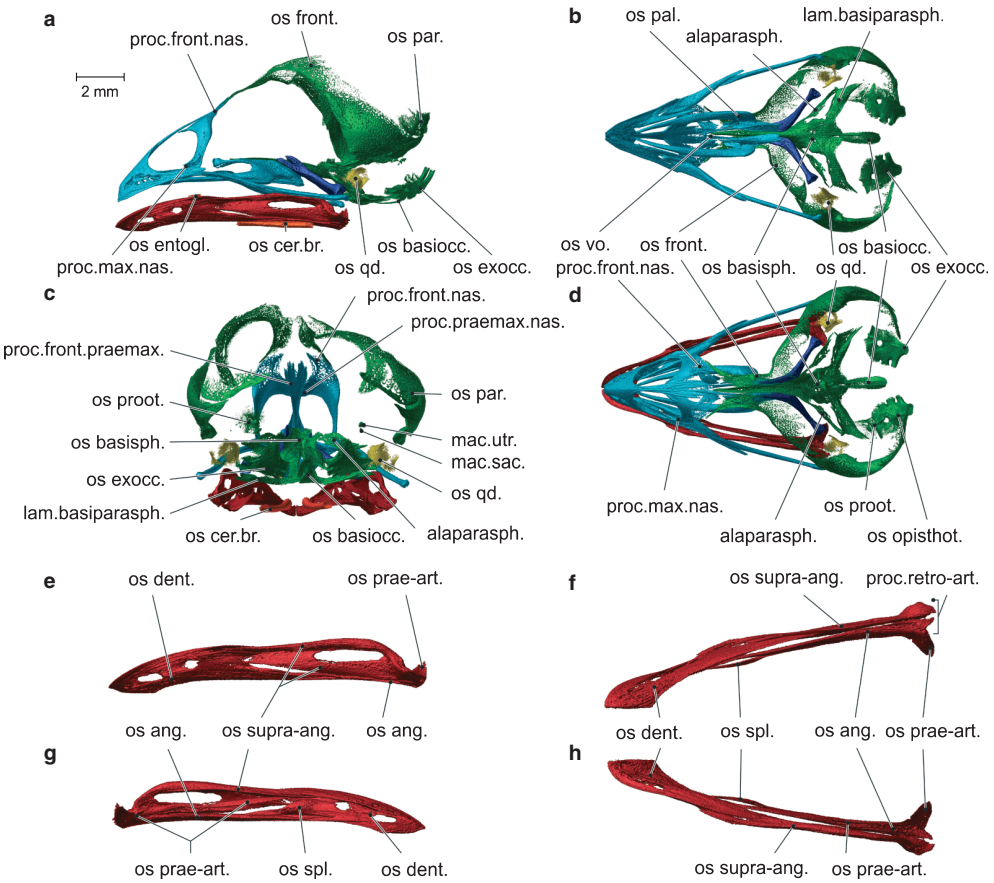

Fig. 4 Lateral view (a), ventral view (without lower jaw) (b), caudal view (c) and dorsal view (d) of the skull of embryo 3, and lateral view (e), ventral view (f), medial view (g) and dorsal view (h) of the left ramus of the lower jaw of embryo 3. Note that several bones of the braincase have started to ossify, and that a first ossification of the os quadratum can be observed. alaparasph., alaparasphenoidale; lam.basiparasph., lamina basiparasphenoidalis; mac.sac., macula sacculi; mac.utr., macula utriculli; os ang., os angulare; os basiocc., os basioccipitale; os basisph., os basisphenoideum; os cer.br., os ceratobranchiale; os dent., os dentalis; os entogl., os entoglossum; os exocc., os exoccipitale; os front., os frontalis; os opisth., os opisthoticum; os par., os parietale; os prae-art., os prae-articulare; os proot., os prooticum; os qd., os quadratum; os spl., os spleniale; os supra-ang., os supra-angulare; proc.front.max., processus frontalis maxillae; proc.front.nas., processus frontalis nasalis; proc.max.nas., processus maxillaris nasalis; proc.max.nas., processus maxillaris nasalis; proc.praemax.nas., processus praemaxillaris nasalis; proc.retro-art., processus retro-articulare.

and sacculi, the os prooticum has started to form. The os basisphenoidale has grown and has fused with the os parasphenoidale. The latter has developed a paired wing at its base, running laterocaudally (the alaparasphenoid) (Figs 4 and 9; Tables 2 and 3).

The processus frontalis praemaxillae has thickened and extends further dorsocaudally. The processus praemaxillaris nasalis has grown more rostrally and somewhat ventral to the processus frontalis praemaxillae. The os nasalis has developed a caudally pointing processus frontalis on its dorsal side and a rostrally pointing processus maxillaris, running medially to the processus maxillaris praemaxillae and laterodorsal to the os maxillare on its ventral side. The processus praemaxillaris maxillae extends more rostrally compared with the previous stage examined.

The dorsocaudal edge of the os palatinum has started to form a platform in which the lateral rostrodorsal spine of the os pterygoideum rests. Ventrocaudal to the rostrodorsal spine the start of the formation of a processus pterygoideus can be observed. The rostral spines on the ventral side of the os palatinum and the processus choanalis rostralis are more developed. The lateral sides of the os vomer have grown out dorsally and its proximal ends now extend more caudally.

The pes pterygoidei now extends more rostrally. The processus quadraticus pterygoidei has thickened and is more spherical. In this specimen, a first perichondral ossification of the os quadratum is visible, specifically the corpus quadrati.

The os spleniale has grown into a thin plate. The rostral part of the os prae-articulare is now visible as a slender plate that runs rostrodorsally, laterodorsal to the os spleniale and ventromedial to the processus dorsalis dentalis. The caudal end of the os prae-articulare and the os angulare have fused and are now indistinguishable.

The os ceratobranchiale has elongated and rostral to it the newly formed os entoglossum appears as two small ossifying bars of a perichondral origin.

Group 2: nestling

Nestling size class 1 – HL 14.9 & 20.6 mm

All the bones of the braincase are now present as the last three bones, the os orbitosphenoidale, the os supraoccipitale and the os mesethmoidale, have started to ossify. The os orbitosphenoidale is positioned ventrocaudally as a round plate lying in line with the os frontale, which has extended medially and caudally. Medioventral to the rostral tips of the os frontale, the os mesethmoidale has started to form. This bone is the last to develop, as it is not present in the 4–5-day-old nestling (DV09E10). The bow-shaped os supraoccipitale is situated along the midline at the back of the braincase, mediodorsal to the os exoccipitale and medioventral to the now enlarged os parietale. The os basioccipitale has ossified more extensively, and its dorsal and ventral sides are now connected. The os prooticum and the os opisthoticum have grown and are fused with each other (ossa otica in Fig. 5) and with the os exoccipitale. Laterally these bones surround the columella auris, and the prooticum encloses the maculae utriculi and saculi. The ossa parasphenoidale and basisphenoidale have grown and enclose the clearly visible sella turcica (Figs 5 and 9; Tables 2 and 3).

In the upper jaw, a ventral floor has formed at the rostroventral tip of the os praemaxillare. The dorsocaudal platform of the os palatinum is more distinct, and a lateral and medial crista have formed. The os quadratum has grown and the corpus quadrati is now fully formed. In the lower jaw, a newly formed perichondral os articulare can be observed, dorsomedial to the caudal end of the os praearticulare. Apart from a general increase in size, no major changes can be observed in the upper jaw, the os vomer, the os palatinum, the os pterygoideum or the lower jaw.

The os entoglossum has become elongated. In one specimen (DV09E02) the os urohyale has started to develop between the two ossa ceratobranchialia (Table 2). In another specimen (DV09E05), a first ossification of the os basihyale is observed between the ossa entoglossa, while no ossification of the os urohyale could be observed (Table 2). In the specimen illustrated in Fig. 5, no signs of ossification of either of these bones can be observed. Hence, it seems that the os urohyale and os basihyale likely ossify nearly simultaneously.

Nestling size 2 – HL 22.8 mm

In this stage several fusions between the bones of the braincase can be observed. The os frontale is starting to fuse with the os orbitosphenoidale and the os squamosum. The latter shows the onset of its fusion with the os parietale. These fusions are not complete, and the sutures between the different bones are still clearly visible. The os parietale now also makes contact with the os supraoccipitale, but no signs of fusion can be observed. All the bones that make up the base of the braincase, i.e. the os parasphenoidale, the os basisphenoidale, the os opistoticum, the os prooticum, the os basioccipitale and the os exoccipitale have fused, and the elements can barely be distinguished from one another. The shape of the upper jaw, the os vomer, the os palatinum, the os pterygoideum and the os quadratum has remained unchanged. There is a strong contact between the bones of the upper jaw, but no fusions have yet taken place. The os vomer and the os palatinum also make intimate contact but have not yet fused (Figs 6 and 9; Tables 2 and 3).

The bones of the lower jaw have grown and are all in intimate contact with each other.

The os basihyale and os urohyale are both present and have ossified further. The os basihyale lies now as a central unit between the two ossa entoglossa. The os urohyale is now a rod-like central unit situated between the distal ends of the ossa ceratobranchialia.

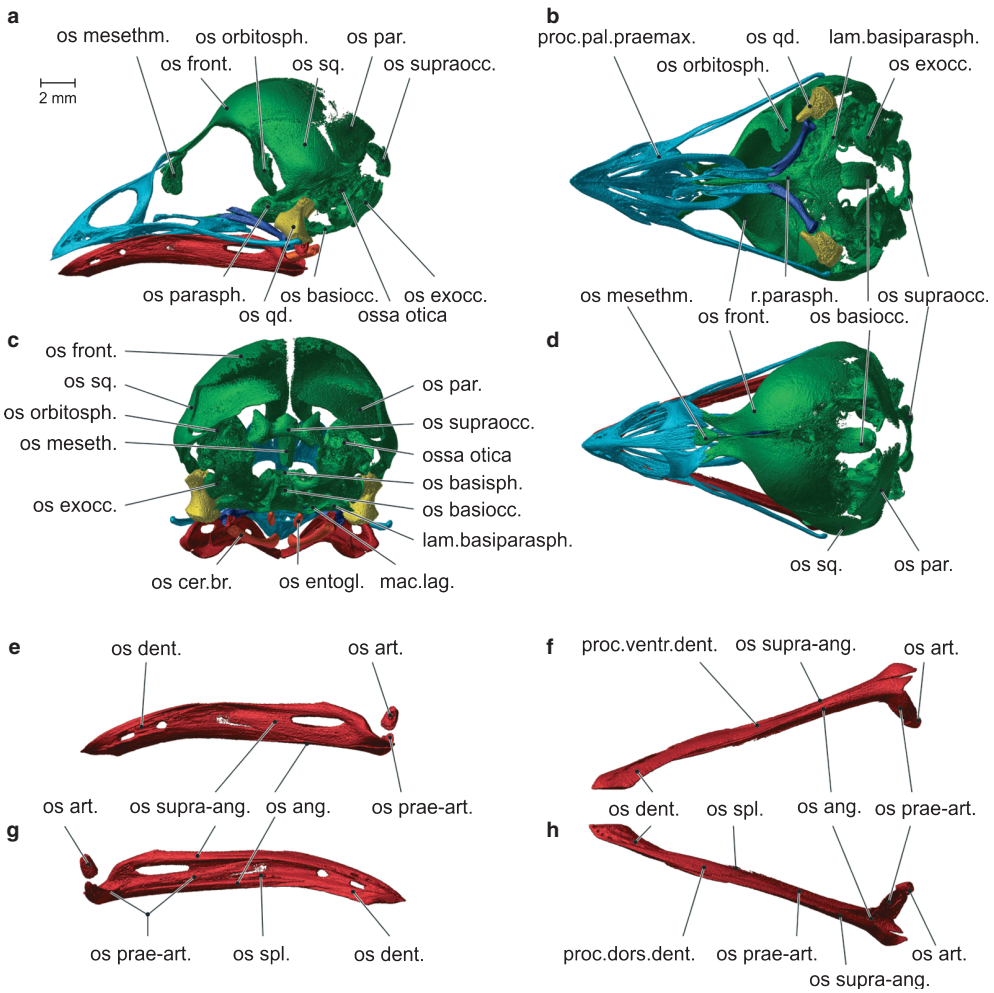

Fig. 5 Lateral view (a), ventral view (without lower jaw) (b), caudal view (c) and dorsal view (d) of the skull of nestling 1, and lateral view (e), ventral view (f), medial view (g) and dorsal view (h) of the left ramus of the lower jaw of nestling 1. Note that all the bones of the braincase have been formed and the os articulare has started to ossify. lam.basiparasph., lamina basiparasphenoidalis; mac.lag., macula lagenae; os ang., os angulare; os art., os articulare; os basiocc., os basioccipitale; os cer.br., os ceratobranchiale; os dent., os dentale; os entogl., os entoglossum; os exocc., os exoccipitale; os front., os frontale; os meseth., os mesethmoideum; os orbitosph., os orbitosphenoideum; os parasph., os parasphenoidale; os prae-art., os prae-articulare; os qd., os quadratum; os spl., os spleniale; os sq., os squamosum; os supra-ang., os supra-angulare; os supraocc., os supraoccipitale; proc.dors.dent., processus dorsalis dentalis; proc.pal.praemax., processus palatinus praemaxillae; proc.ventr.dent., processus ventralis dentalis; r.parasph., rostrum parasphenoidale.

Group 3: juvenile

Juvenile size class 1 – HL 31.7–32.0 mm

In the braincase, all the bones now have fused, with a newly formed septum interorbitale present between the os frontale, the os mesetmoidale and the os parasphenoidale. The rostral ends of the ossa frontalia have fused with the caudal ends of the processus frontalis praemaxillae et nasalis, forming a flexion zone between the upper beak and the braincase, also called the frontonasal hinge (i.e. zona flexoria arcus cranio facialis). Four processes have developed, i.e. from dorsal to ventral: the processus postorbitalis; the processus zygomaticus; the processus suprameaticus; and the processus paroccipitalis. On the lateral side of the braincase a distinct crista temporalis can be seen. This crista borders the large, lateral fossa temporalis. On the caudal side of the braincase, another crista is present now, i.e. the crista nuchalis transversa (Figs 7 and 9; Tables 2 and 3).

All the bones of the upper jaw now have fused completely. In addition to the frontonasal hinge, two other flexion zones can be observed: a zona flexoria arcus jugalis situated where the jugal bar meets the upper beak; and a zona flexoria palatina positioned between the upper beak and the processus praemaxillaris palatini. Ventral to the processus frontalis praemaxillae the septum nasalis is now visible. A processus transpalatinus has developed at the ventrocaudal end of the os palatinum. On the dorsal side of the processus quadraticus of the os pterygoideum a distinct processus dorsalis can now be observed.

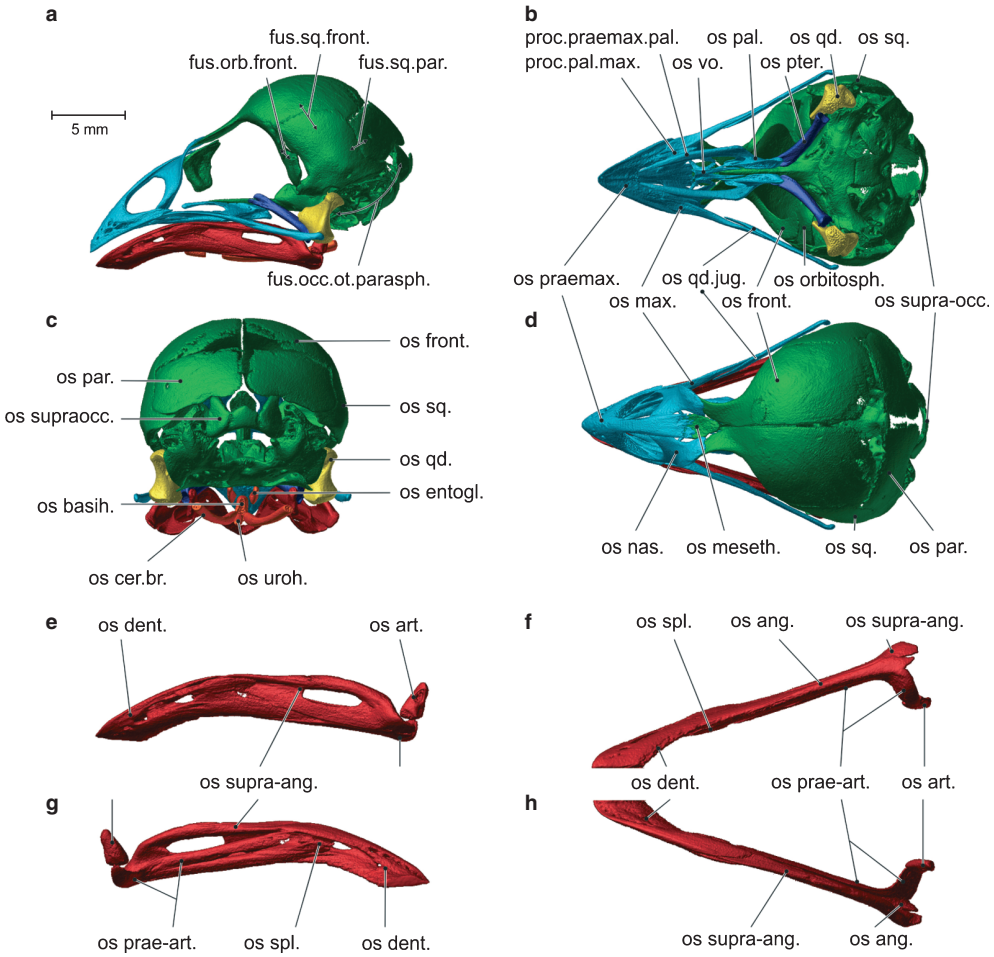

Fig. 6 Lateral view (a), ventral view (without lower jaw) (b), caudal view (c) and dorsal view (d) of the skull of nestling 2, and lateral view (e), ventral view (f), medial view (g) and dorsal view (h) of the left ramus of the lower jaw of nestling 2. fus.occ.ot.parasph., fussion occipital region ossa otica os parasphenoidale; fus.orb.front., fussion os orbitosphenoidale os frontale; fus.sq.front., fussion os squamosum os frontale; fus.sq.par., fussion os squamosum os parietale; os ang., os angulare; os art., os articulare; os basih., os basihyale; os cer.br., os ceratobranchiale; os dent., os dentale; os entogl., os entoglossum; os front., os frontale; os max., os maxillare; os meseth., os mesethmoideum; os nas., os nasale; os orbitosph., os orbitosphenoidale; os pal., os palatinum; os par., os parietale; os prae-art., os prae-articulare; os praemax., os praemaxillare; os pter., os pterygoideum; os qd.jug., os quadratojugale; os spl., os spleniale; os sq., os squamosum; os supra-ang., os supra-angulare; os supraocc., os supraoccipitale; os supraocc., os supraoccipitale; os uroh., os urohyale; os vo., os vomer; proc.praemax.pal., processus preamaxillaris palatini; proc.pal.max., processus palatinus maxillae.

On the os quadratum three processes have developed: a dorsal processus oticus, which articulates with the processus suprameaticus of the braincase; a mediorostral processus orbitalis for muscle attachment of the musculi adductor mandibulae ossis quadrati and pseudotemporalis profundus; and a ventral processus mandibularis, which articulates with the processus quadraticus pterygoidei through a condylus pterygoideus, with the condylus quadraticus of the jugal bar through the cotyla quadratojugalis, and with the lower jaw through the condyli lateralis, medialis and caudalis.

All bones of the lower jaw now are also fully fused, with two parts remaining visible: a pars dentalis and a pars caudalis. Both parts have become more robust, and three processes can be distinguished in the pars caudalis: the processus coronoideus, which consists of two dorsal tubercles; the processus mandibulae medialis; and the processus mandibulae lateralis with a condylus caudalis and a condylus lateralis. Also a tuberculum pseudotemporalis is clearly visible mediocaudal to the second tubercle of the processus coronoideus.

Some new, small bones have developed close to the quadratomandibular joint. They are sesamoid bones that are formed in the ligamentum jugomandibularis medialis.

The os basihyale now is a laterally flattened plate, situated at the midline. At its distal end it articulates with the ossa entoglossa that lie lateral to it as two parallel splints of bone. Caudally, the os basihyale has fused with the os urohyale. At the place of fusion, the os basihyale articulates with the ossa ceratobranchialia. Caudal to the os cerato-

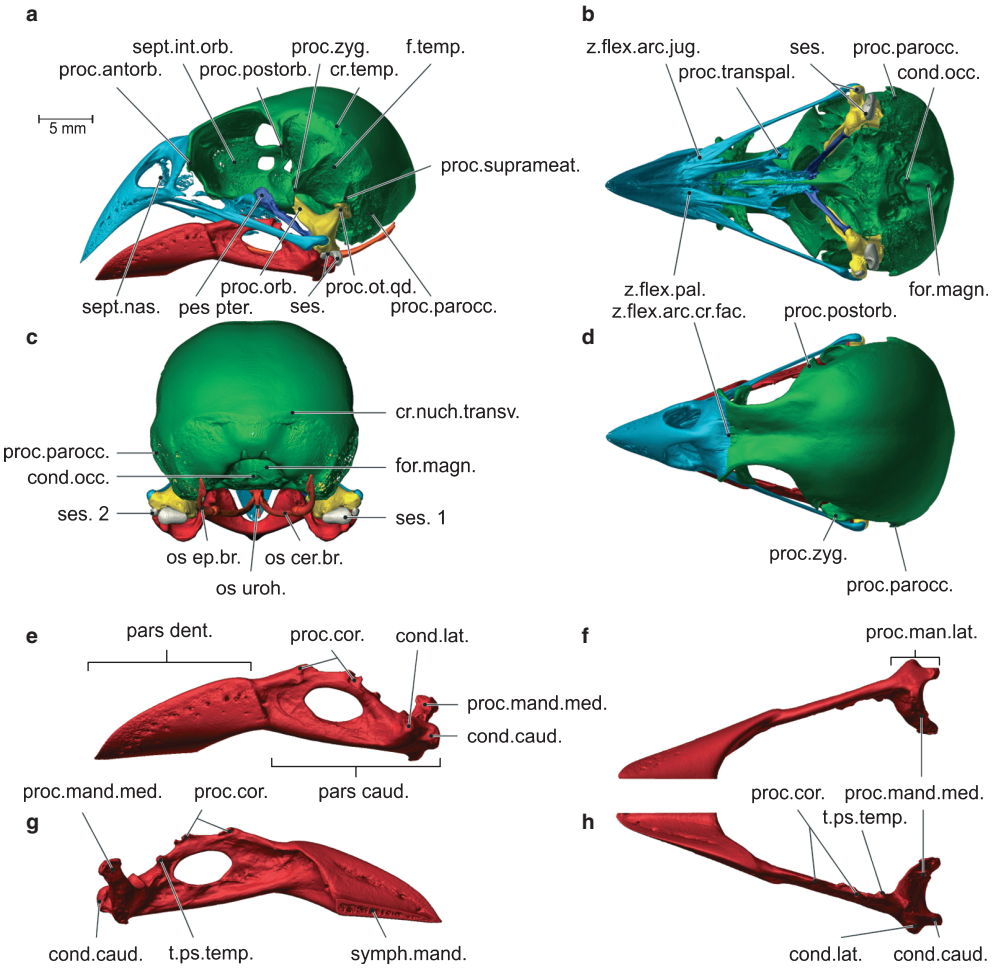

Fig. 7 Lateral view (a), ventral view (without lower jaw) (b), caudal view (c) and dorsal view (d) of the skull of juvenile 1, and lateral view (e), ventral view (f), medial view (g) and dorsal view (h) of the left ramus of the lower jaw of juvenile 1. Note the formation of cristae and processes, especially on the lateral side of the braincase and on the lower jaw. cond.caud., condilus caudalis; cond.lat., condylus lateralis; cond.occ., condylus occipitalis; cr.temp., crista temporalis; cr.nuch.transv., crista nuchalis transversa; f.temp., fossa temporalis; for.magn., foramen magnum; pars caud., pars caudalis; pars dent., pars dentalis; pes pter., pes pterygoidei; proc. parocc., processus paroccipitalis; proc.antorb., processus antorbitalis; proc.cor. processus coronoideus; proc.mand.lat., processus mandibulae lateralis; proc.mand.med., processus mandibulae medialis; proc.orb., processus orbitalis; proc.ot.qd., processus oticus quadrati; proc.postorb., processus postorbitale; proc.suprameat., processus suprameaticus; proc.zyg., processus zygomaticus; sept.int.orb., septum interorbitale; sept.nas., septum nasalis; ses. 1, large sesamoid bone; ses. 2, small sesamoid bone; symph.mand., symphysis mandibulae; t.ps.temp., tuberculum pseudotemporalis; z.flex.arc.cr.fac., zona flexoria arcus cranio facialis; z.flex.arc.jug., zona flexoria arcus jugalis; z.flex.pal., zona flexoria palatina.

branchiale lies the newly formed, bar-like os epibranchiale with which it articulates. All hyoid bones bear strongly developed cristae.

Group 4: adult

Adult – HL 31.59–33.71 mm

All the parts of the skull have grown further and have become more robust. The crista temporalis and the processus zygomaticus have become more developed, and the fossa temporalis has extended further dorsocaudally. In the lower jaw, the processus coronoideus has grown taller and has become more robust, and several cristae are formed on the lateral and medial side of the pars caudalis. For a full description of the cranial osteology of an adult *Geospiza fortis* we refer to Genbrugge et al. (submitted) (Figs 8 and 9; Tables 2 and 3).

Morphometry

Upper jaw–braincase–pterygoid–palatine–quadrate complex

This analysis shows that the first shape axis explains 82.73% of the variation. Together with the second axis more than 90% of the variation in shape is explained. The first axis reflects variation in the position of the upper beak, shifting

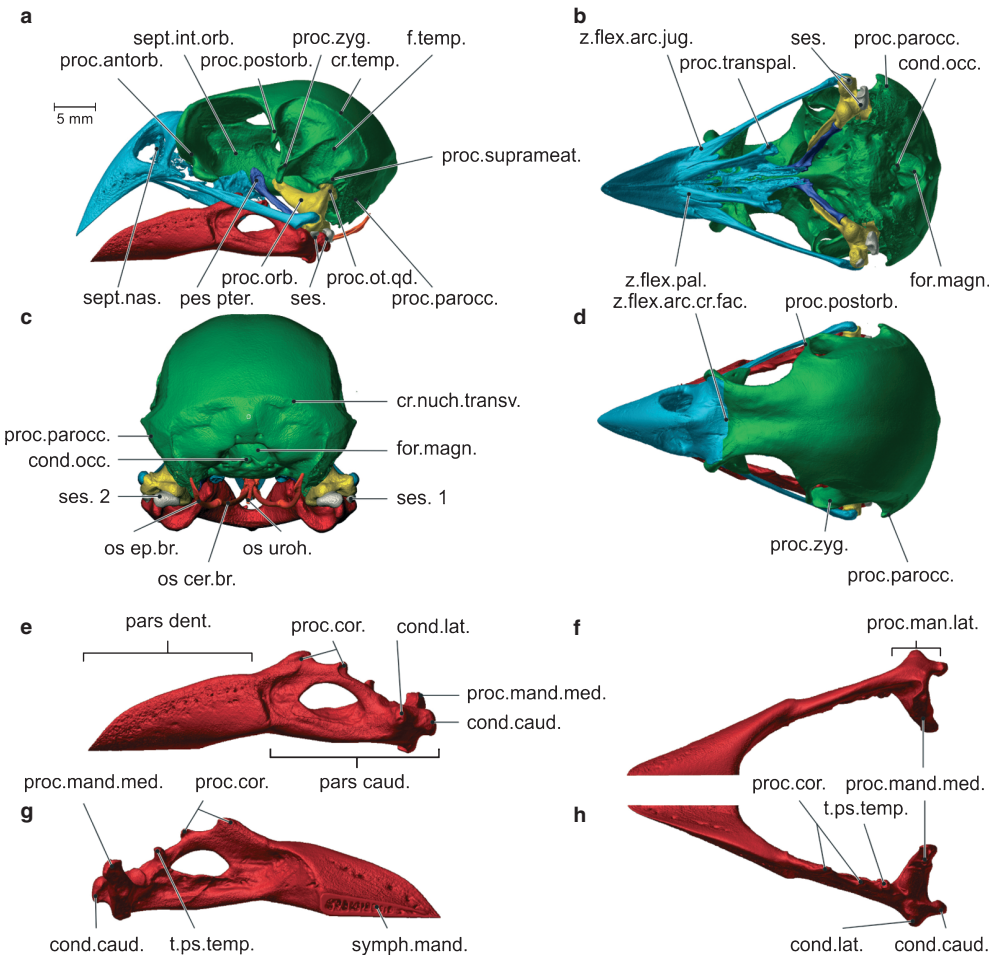

Fig. 8 Lateral view (a), ventral view (without lower jaw) (b), caudal view (c) and dorsal view (d) of the skull of adult 1, and lateral view (e), ventral view (f), medial view (g) and dorsal view (h) of the left ramus of the lower jaw of adult 1. Note that the cristae and processes have become more developed. cond.caud., condylus caudalis; cond.lat., condylus lateralis; cond.occ., condylus occipitalis; cr.temp., crista temporalis; cr.nuch.transv., crista nuchalis transversa; f.temp., fossa temporalis; for.magn., foramen magnum; pars caud., pars caudalis; pars dent., pars dentalis; pes pter., pes pterygoidei; proc.antorb., processus antorbitalis; proc.cor., processus coronoideus; proc.mand.lat., processus mandibulae lateralis; proc.mand.med., processus mandibulae madialis; proc.orb., processus orbitalis; proc.ot.qd., processus oticus quadrati; proc.parocc., processus paroccipitalis; proc.postorb., processus postorbitalis; proc.suprameat., processus suprameaticus; proc.transpal., processus transpalatinus; proc.zyg., processus zygomaticus; sept.in.orb., septum interobitalis; sept.nas., septum nasalis; ses. 1, large sesamoid bone; ses. 2, small sesamoid bone; ses., sesamoid bones; symph.mand., symphysis mandibulae; t.ps.temp., tuberculum pseudotemporalis; z.flex.arc.cr.fac., zona flexoria arcus cranio facialis; z.flex.arc.jug., zona flexoria arcus jugalis; z.flex.pal., zona flexoria palatina.

from a horizontal position to a more vertical one as the finches grow older. Associated with this, the angle between the upper beak and the jugal bar and palatine increases. Additionally, a shift of the skull table to a more horizontal orientation can be observed, thereby pulling the orbit forwards and upwards. A division of the specimens along the second axis is clearly visible, with the embryo and nestlings on the left, and the juvenile and adult on the right, illustrating that a remarkable shape change takes place during the transition of the nestling to the juvenile period (Fig. 10).

Lower jaw

In the analysis of the lower jaw 74.92% of the shape change is described by the first axis. This axis summarizes the heightening of the lower jaw, especially at the level of the processus coronoideus. Another 20.17% is explained by the second axis, which mainly describes the shape changes in the os articulare and the processus mandibulae medialis, and the change in angle between the pars dentalis and the pars caudalis. This angle is greatest in the second nestling, but then decreases again towards the final stages of development (Fig. 11).

Discussion

Although Darwin's finches have been the subject of many studies in ecology and evolution, including eco-morphology (Bowman, 1961; Boag & Grant, 1981; Schluter, 1982; Grant,

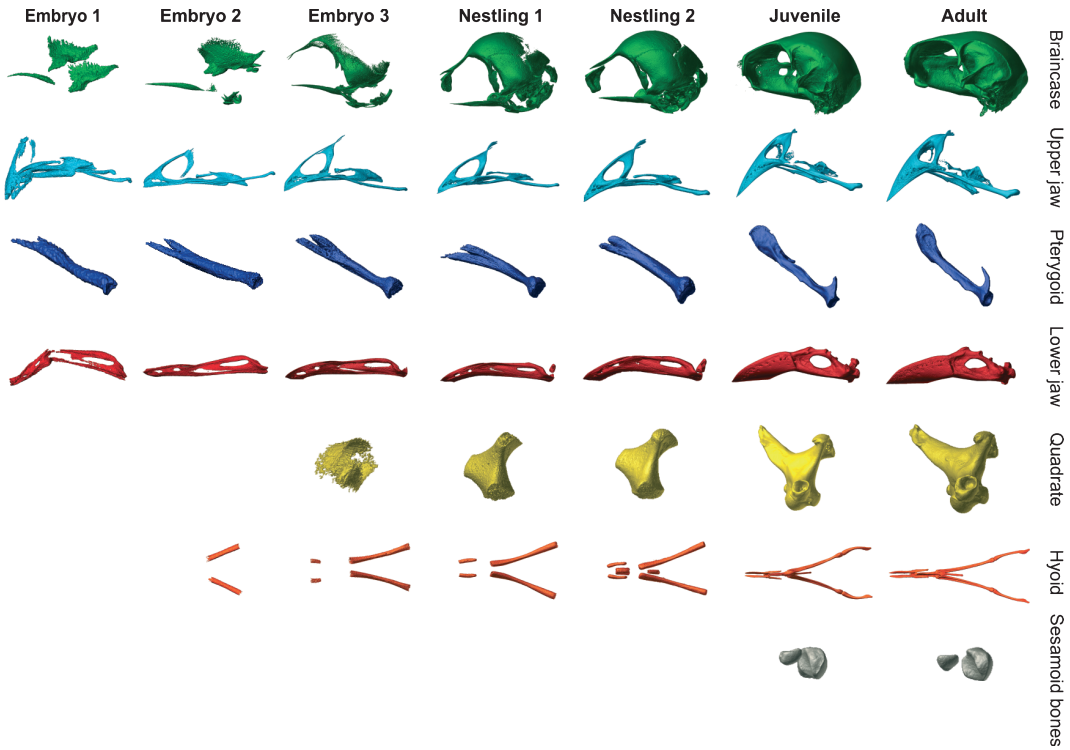

Fig. 9 Overview of the development of the different parts of the skull of the seven specimens described in this study. Parts are shown in lateral view, except the hyobranchial apparatus, which is shown in dorsal view. Note the cristae and processes present in the juvenile and the adult.

1986; Herrel et al. 2005a,b; Grant & Grant, 2008), song characteristics and evolution (Goodale & Podos, 2010; Podos, 2010), phylogenetic affinity (Price & Grant, 1985; Petren et al. 1999; Sato et al. 1999; Price et al. 2009) and early development (Abzhanov et al. 2004, 2006), surprisingly little is known about the ontogeny and ossification of the cranium, mandible and hyobranchial apparatus. A comparison of the specimens included in this study, ranging from embryos up to adults, illustrates the often dramatic changes in shape and development of processes and cristae that occurs during the later stages of development.

The first bones to develop are those that will comprise the upper and lower beak, the os pterygoideum and the os palatinum. Next, the braincase, the os quadratum and the small sesamoid bones start to form. The embryonic period is typically characterized by the initial ossification of the different bony elements of the skull. From the nestling period onwards, all the bones are present, followed by further growth and subsequent fusion between them. In the juvenile and adult periods fusion is complete, with the cristae and processes that serve as muscle attachment sites having been formed on the braincase. Unexpectedly, the greatest

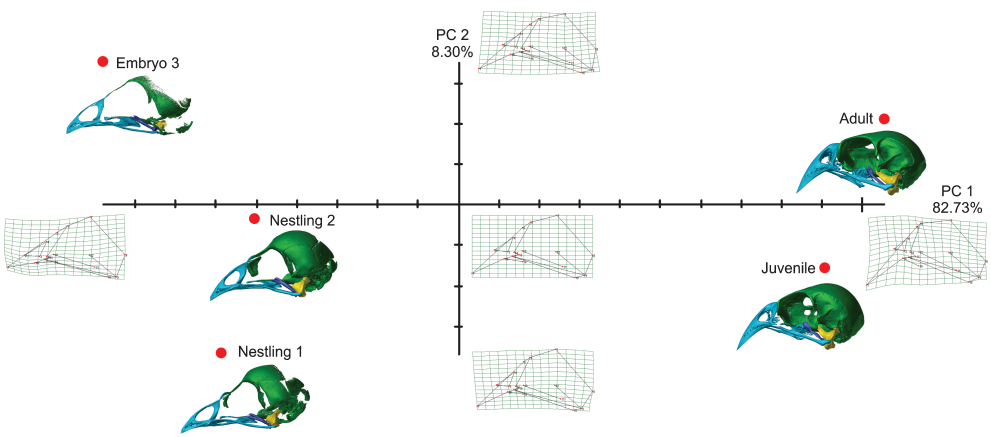

Fig. 10 Graphical illustration of the geometric morphometric analysis of the late embryo, the nestlings, the juvenile and adult. Note that the first shape axis explains most of the shape variation.

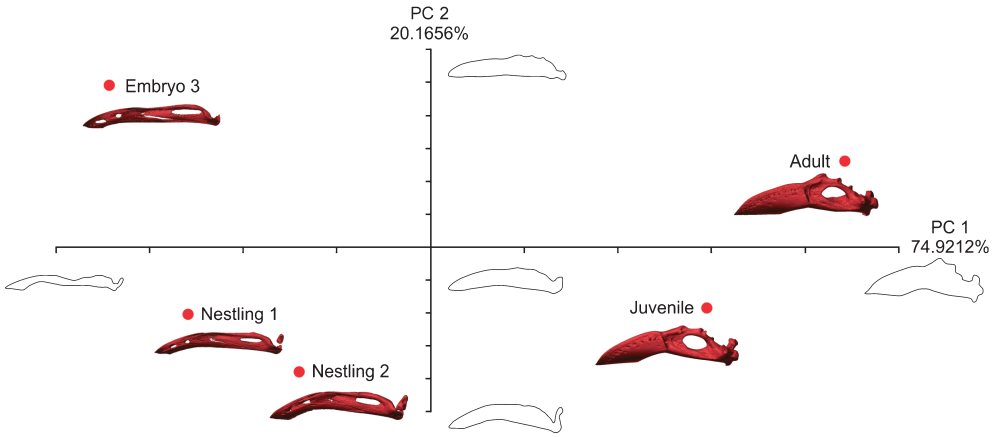

Fig. 11 Graphical illustration of the Fourier analysis of the late embryo, the nestlings, the juvenile and adult. Note that the first shape axis explains most of the shape variation.

changes in head shape, as indicated by our geometric morphometric analysis, can be observed between the nestling and juvenile specimens. This transition corresponds to a significant change in diet and feeding behavior: nestlings' diet consists of soft food (caterpillars and small spiders; Boag & Grant, 1984) from their parents, whereas juvenile birds start to eat and crack harder food items such as seeds. The cristae and processes involved in cracking food items become even more robust in the adult, forming additional attachment sites for the large jaw adductor muscles (Bowman, 1961; Genbrugge et al. submitted). The processus zygomaticus and the crista temporalis are particularly prominent and serve as attachment sites for the musculus adductor mandibulae externus (Bowman, 1961; Genbrugge et al. submitted). The formation of cristae and processes in the transition from juvenile to adult is also very visible in the lower jaw, where the prominent processus coronoideus and tuberculum pseudotemporalis are formed and serve as insertion sites for the adductor muscles (Bowman, 1961, Genbrugge et al. submitted).

The formation of cristae and processes between our nestling and juvenile stage can also be observed in the other skeletal elements of the head. The os palatinum develops a robust processus transpalatinus with a strong crista running around its ventrocaudal end associated with the insertion of the strong aponeurosis of the pterygoideus muscle complex (Bowman, 1961; Genbrugge et al. submitted). The os pterygoideum has developed long cristae along its corpus, which serve as additional attachment sites for the muscles pterygoideus dorsalis medialis (Bowman, 1961; Genbrugge et al. submitted). Moreover, a dorsal process develops on the processus quadratus of the os pterygoideum, upon which the musculus protractor pterygoidei et quadrati attaches (Bowman, 1961; Genbrugge et al. submitted). The important impact of muscle contraction on the formation of bone and the overall structure of the skull has been demonstrated in other birds such as African Seedcrackers (Clabaut et al. 2009), where the development of the jaw adductor muscles is hypothesized to drive differences in cranial size and shape. The observed shape changes in the growth of the skull in the medium ground finch between nestling and adult may partly explain the exceptional variability observed in adult morphology in this species, even within populations (Grant, 1986).

In addition to the formation of these processes and cristae, some skeletal elements shift throughout ontogeny. In the braincase, the os frontale changes its orientation from a diagonal position in the late embryo stage to an almost horizontal position in the adult, thus raising the orbit. The eyes thus stay in line with the tomial ridges of the rotated upper jaw (discussed below), and more space is available ventral and caudal to the eye for muscle enlargement and attachment (Bowman, 1961). The caudal end of the upper jaw follows the upwards shift of the os frontale, and changes its position from nearly horizontal to form an increasingly sharper angle between the upper beak and the jugal bar and palate. Consequently, the bony upper beak, the jugal bar and the palate become positioned more vertically. In that way, the position of the palate matches the line of action of the pterygoid muscles (Bowman, 1961), which is likely facilitates effective force transmission during the cracking of hard seeds.

The lower jaw forms an angle caudally between its pars rostralis and pars caudalis, which is greatest in the juvenile but attenuates in the adult as the lower jaw becomes more robust. The pars caudalis increases in thickness and depth, creating more attachment surface area for the pterygoid muscles and the musculus pseudotemporalis profundus on the medial side, and for the ventral part of the musculus adductor mandibulae externus complex (Bowman, 1961). The change in these angles in the upper and lower jaw changes their relative position, giving the impression that a space remains between upper and lower jaws. Strong rims of keratin on the tomial cristae fill this gap, however.

The sesamoid bones are formed after the birds leave the nest. Although their function remains unclear, tendinous ossifications typically arise where tendons are in compression (Benjamin & Ralphs, 1998). Thus, the posterior part of the quadratomandibular joint and the associated tendons may be loaded in compression when birds start to feed on harder food items.

Comparative analysis of the ossification sequence

Compared with the cranial skeletal ontogeny of the chicken (*Gallus gallus domesticus*) and other neognathous birds, some differences can be observed in *Geospiza fortis*. For example, in the braincase of *G. fortis,* several bones such as the os prefrontale and os ectethmoidale (latero-ethmoidale) were not observed to develop. However, it is possible that these bones develop between the nestling and juvenile stages studied, as Jollie (1957) states that these bones appear late in development, and that these are already fused and thus undistinguishable in the braincase of the juvenile. An os jugale is also lacking between the os maxillare and the os quadrato-jugale. This bone is, however, present in the chicken, already from an early stage of development, and is also observed in other birds such as bee-eaters (*Merops* sp.; Brusaferro & Simonetta, 1998). On the other hand, the os jugale is known to be absent in several other bird species, such as the magpie (*Pica pica*), the English sparrow (*Passer domesticus*), the robin (*Turdus migratorius*) and the kestrel (*Falco tinnunculus*; Jollie, 1957).

The os pterygoideum has two rostrodorsal spines, but due to the lack of specimens representing a stage between the nestling and the juvenile stages, no clear description can yet be given about what happens with these two parts in *G. fortis*. According to the literature (Jollie, 1957; Baumel et al. 1979; Zusi & Livezey, 2006), the medial, rostrodorsal part is thought to develop as the pes pterygoidei and the lateral part is thought to fuse with the dorsal edge of the os palatinum, while an articulation would arise between the two parts. In the chicken, Jollie (1957) describes the formation of an os 'pterygopalatinum', being the rostral part of the os pterygoideum that immediately fuses with the os palatinum at an early stage of development.

The os articulare develops late during development in *Geospiza fortis* as a perichondral bone. It does not immediately fuse with the os prae-articulare, which has been described for the chicken, but stays separate, as has been observed for the English sparrow (Jollie, 1957). Only later, during the transition of nestling to juvenile, does it fuse with the os prae-articulare. The long but slender os prae-articulare extends for almost along the half of the length of the lower jaw, as in most birds. The chicken, with its short prae-articulare, is unusual in that way (Jollie, 1957).

Conclusion

Our data show that the greatest changes in skull shape appear between nestling and juvenile stages. The reorientation of the beak and the orbit, and the formation of well-developed processes and cristae between our nestling and juvenile stages seem to support our hypothesis that these changes are related to the active feeding of the birds after leaving the nest. This suggests that, in addition to the well-documented genetic determination of beak size, the active use of the jaw muscles during seed cracking may potentially play an important role in shaping adult skull morphology. Investigating the development of the jaw muscles and their interaction with the observed ossification and formation of the skull and lower jaw would make an important complement to this study.

Acknowledgements

Fieldwork was coordinated through the Charles Darwin Research Station and the Galápagos National Park Service. The authors thank Eric Hilton, Sarah Huber and Bieke Vanhooydonck for their assistance in the field, and for helping collect road-killed specimens. This work was supported by NSF grant IBN-0347291 to J.P., by an interdisciplinary research grant of the special research fund of the University of Antwerp to P.A., J.D., A.G. and A.H., and by a PHC Tournesol collaborative grant to D.A. and A.H. The UGCT scanning facility acknowledges the support from the Ghent University special research fund (BOF).

Author contributions

CT scanning: Matthieu Boone, Luc Van Hoorebeke; acquisition of material: Anthony Herrel, Jeffrey Podos; drafting of the manuscript: Annelies Genbrugge; interpretation of CT scans: Annelies Genbrugge, Anne-Sophie Heyde; methods: Dominique Adriaens, Peter Aerts, Anthony Herrel; critical revision of the manuscript: all authors.

References

Abzhanov A, Protas M, Grant BR, et al. (2004) Bmp4 and morphological variation of beaks in Darwin's finches. *Science* **305**, 1462–1464.

Abzhanov A, Kuo WP, Hartmann C, et al. (2006) The calmodulin pathway and evolution of the elongated beak morphology in Darwin's finches. *Nature* **442**, 563–567.

Baumel JJ, King AS, Lucas AM, et al. (1979) *Nomina Anatomica Avum*. London: Academic Press, pp. 53–219.

Benjamin M, Ralphs JR (1998) Fibrocartilage in tendons and ligaments an adaptation to compressive load. *J Anat* **193**, 481–494.

Boag PT, Grant PR (1981) Intense natural selection in a population of Darwin's finches (Geospizinae) in the Galápagos. *Science* **214**, 82–85.

Boag PT, Grant PR (1984) Darwin's finches (*Geospiza*) on Isla Daphne major, Galapagos: breeding and feeding ecology in a climatically variable environment. *Ecol Monogr* **54**, 463–489.

Bowman RI (1961) Morphological differentiation and adaptation in the Galapagos finches. *Univ Calif Publ Zool* **58**, 1–302.

Brusaferro A, Simonetta AM (1998) Morphology of the feeding apparatus in nestlings of *Merops*. *Ital J Zool* **65**, 249–259.

Campàs O, Mallarino R, Herrel A, et al. (2010) Scaling and shear transformations capture beak shape variation in Darwin's finches. *PNAS* **107**, 3356–3360.

Clabaut C, Herrel A, Sanger TJ, et al. (2009) Development of beak polymorfism in the african seedcracker, *Pyrenestes ostrinus*. *Evol Dev* **11**, 636–646.

Darwin CR (1841) *The Zoology of the Voyage of H.M.S. Beagle, Under the Command of Captain FitzRoy R.N. During the Years 1832–1836. Part III: birds*. London: Smith Elder.

Foster DJ, Podos J, Hendry AP (2008) A geometric morphometric appraisal of beak shape in Darwin's finches. *J Evol Biol* **21**, 263–275.

Gibbs HL (1988) Heritability and selection on clutch size in Darwin's medium ground finches (*Geospiza fortis*). *Evolution* **42**, 750–762.

Goodale E, Podos J (2010) Persistence of song types in Darwin's finches, *Geospiza fortis*, over four decades. *Biol Lett* **6**, 589–592.

Grant PR (1981) Patterns of growth in Darwin's finches. *Proc Roy Soc London B* **212**, 403–432.

Grant PR (1986) *Ecology and Evolution of Darwin's Finches*. Princeton, New Jersey: Princeton University Press, 492.

Grant PR, Grant BR (2006) Evolution of character displacement in Darwin's finches. *Science* **313**, 224.

Grant PR, Grant BR (2008) *How and Why Species Multiply: the Radiation of Darwin's Finches*. Princeton, New Jersey: Princeton University Press, 218.

Herrel A, Podos J, Huber SK, et al. (2005a) Bite performance and morphology in a population of Darwin's finches: implications for the evolution of beak shape. *Funct Ecol* **19**, 43–48.

Herrel A, Podos J, Huber SK, et al. (2005b) Evolution of bite force in Darwin's finches: a key role for head width. *J Evol Biol* **18**, 669–675.

Iwata H, Ukai Y (2002) SHAPE: a computer program package for quantitative evaluation of biological shapes based on elliptic Fourier descriptors. *J Heredity* **93**, 384–385.

Jollie MT (1957) The head skeleton of the chicken and remarks on the anatomy of this region in other birds. *J Morphol* **100**, 389–436.

Petren K, Grant BR, Grant PR (1999) A phylogeny of Darwin's finches based on microsatellite DNA length variation. *Proc R Soc Lond B* **266**, 321–329.

Podos J (2010) Acoustic discrimination of sympatric morphs in Darwin's finches: a behavioural mechanism for assortative mating? *Philos Trans R Soc Lond B Biol Sci* **365**, 1031–1039.

Price TD, Grant PR (1985) The evolution of ontogeny in Darwin's finches: a quantitative genetic approach. *Am Nat* **125**, 169–188.

Price TD, Qvarnström A, Irwin DE (2009) The role of phenotypic plasticity in driving genetic evolution. *Proc R Soc Lond B* **270**, 1433–1440.

Rohlf FJ (2003) *tpsSmall: Thin Plate Spline Small Variation Analysis (Version 1.2)*. Stony Brook, New York: State University of New York at Stony Brook.

Rohlf FJ (2010a) *tpsRelw: Thin Plate Spline Relative Warp Analysis (Version 1.49)*. Stony Brook, New York: State University of New York at Stony Brook.

Rohlf FJ (2010b) *tpsDig2: Thin Plate Spline Digitizing Landmarks (Version 2.16)*. Stony Brook, New York: State University of New York at Stony Brook.

Sato A, O'hUigin C, Figueroa F, et al. (1999) Phylogeny of Darwin's finches as revealed by mtDNA sequences. *Proc Natl Acad Sci USA* **96**, 5101–5106.

Schluter D (1982) Seed and patch selection by Galápagos Ground finches: relation to foraging efficiency and food supply. *Ecology* **63**, 1106–1120.

Schluter D (1984) Morphological and phylogenetic relations among Darwin's finches. *Evolution* **38**, 921–930.

Schluter D, Grant PR (1984) Determinants of morphological patterns in communities of Darwin's finches. *Am Nat* **123**, 175–196.

Soons J, Herrel A, Genbrugge A, et al. (2010) Mechanical stress, fracture risk and beak evolution in Darwin's ground finches (*Geospiza*). *Philos Trans R Soc Lond B Biol Sci* **365**, 1093–1098.

Vlassenbroeck J, Dierick M, Masschaele B, et al. (2007) Software tools for quantification of X-ray microtomography at the UGCT. *Nucl Instr Meth Phys Res A* **580**, 442–445.

Zusi RL, Livezey BC (2006) Variation in the os palatinum and its structural relation to the palatinum osseum of birds (Aves). *Ann Carnegie Mus* **75**, 137–180.